

Early-Stage Deforestation Detection in the Tropics With L -band SAR

Manabu Watanabe¹, Senior Member, IEEE, Christian N. Koyama², Member, IEEE, Masato Hayashi, Izumi Nagatani³, and Masanobu Shimada, Fellow, IEEE

Abstract—Polarimetric characteristics of early-stage deforestation areas were examined with L -band synthetic aperture radar (SAR) to develop a forest early warning system. Time series of PALSAR-2/ScanSAR data and Landsat data were used to examine the differences in detection timing of deforestation in the most active deforestation sites in Peru and Brazil. The γ^0_{HH} value increased by 0.8 dB on average for areas undergoing early-stages of deforestation, in which felled trees were left on the ground. The detection timing was almost the same as that of using the optical sensor. On the other hand, the γ^0_{HV} value does not show significant γ^0 change at this early-stage of deforestation. The γ^0_{HV} value started to decrease 1–1.5 months after the deforestation was detected by Landsat. The γ^0_{HV} value decreased by 1.5–1.6 dB, 4–5 months after the deforestation. To understand the radar backscattering mechanism at the early-stage deforestation sites, field experiments were carried out 2–16 days after the PALSAR-2/fully-polarimetric observations. The early-stage deforestation sites revealed 1.1–2.5 dB and 2.9–4.0 dB increases for σ^0_{HH} and $\sigma^0_{surface}$, respectively. This can be explained by the direct (single bounce) scattering from felled trees left on the ground. The sites in which felled trees were removed and the surfaces were flattened showed 5.2–5.3 dB and 5.3–5.5 dB decreases for σ^0_{HV} and σ^0_{volume} , respectively. This can be explained by the lower sensitivity of the HV polarization to both the branches remaining on the ground and the surface roughness, along with its increased sensitivity to the forest biomass. We conclude that an increase in L -band γ^0_{HH} is a good indicator for detecting early-stage deforestation sites, where felled trees are left on the ground, while γ^0_{HV} may be useful for detecting later-stage deforestation sites.

Index Terms—Forest monitoring, PALSAR-2, polarization, polarimetric decomposition.

I. INTRODUCTION

THE Intergovernmental Panel on Climate Change has determined that land use change, including decreasing amounts of forest area, is an important factor in global climate change [1].

Manuscript received September 15, 2017; revised January 30, 2018; accepted February 11, 2018. Date of publication March 28, 2018; date of current version June 29, 2018. This work was supported by the research budget of JAXA. The results will be used for early deforestation detection in global tropical forests by the JJ-FAST system, funded by JICA and JAXA. (Corresponding author: Manabu Watanabe.)

M. Watanabe and C. N. Koyama are with the School of Science and Engineering, Tokyo Denki University, Hiki-gun 350-0394, Japan (e-mail: 16hz001@ms.dendai.ac.jp; 16hz010@ms.dendai.ac.jp).

M. Hayashi and I. Nagatani are with the Earth Observation Research Center, Japan Aerospace Exploration Agency, Tsukuba-shi 305-8505, Japan (e-mail: hayashi.masato2@jaxa.jp; nagatani.izumi@jaxa.jp).

M. Shimada is with the School of Science and Engineering, Tokyo Denki University, Hiki-gun 350-0394, Japan, and also with the Earth Observation Research Center, Japan Aerospace Exploration Agency, Tsukuba-shi 305-8505, Japan (e-mail: shimada@g.dendai.ac.jp).

Digital Object Identifier 10.1109/JSTARS.2018.2810857

Satellite data plays an important role in global forest monitoring and deforestation detection [2].

Several global/country level deforestation monitoring systems based on the optical satellite data are working. Forest Alerts dataset of Global Land Analysis & Discovery (GLAD, [3], [4]) uses Landsat data and covers Peru, Brazil, central Africa, and a part of South Asia. The PRODES [5], [6] is the deforestation monitoring system in the Brazilian Amazon since 1988. Deforestation map is produced by visual interpretation of different optical images, with spatial and spectral resolution similar to those of LANDSAT5/TM with minimum area of 6.25 ha. GEO bosques [7] is an information service that develops and provides the national program for conservation of forests in Peru. The service includes early warning monitoring performed in near real-time with data reported every 7 days and the spatial resolution is 30 m, achieving thus detect losses of forest from 0.09 ha. However, cloud cover often disturbs early deforestation detection, especially during the rainy season.

Synthetic aperture radar (SAR) observations are available for all weather conditions, day and night, and can create an especially effective early warning system for deforestation. In the Brazilian Amazon, between 2009 and 2012, the Japan International Cooperation Agency (JICA) and the Japan Aerospace Exploration Agency (JAXA) supported the monitoring and detection of illegal logging in near real-time, using observational data from Advanced Land Observation Satellite (ALOS). More than 2000 illegal logging incidents were detected, which greatly contributed to a 39.9% reduction in deforestation between 2007 and 2010 [5]. As a result, JICA and JAXA launched a new system, JICA-JAXA Forest Early Warning System in the Tropics (JJ-FAST), in November 2016 [8]. The system is accessible online from smartphones and other devices. It is based on the monitoring of data related to deforestation and forest changes in tropical regions, which can be found in 77 countries. Users can freely download not only for deforestation polygons detected by PALSAR-2, but also the orthorectified tile image before and after the deforestation near the deforestation area. The tile image currently includes only HV polarization, and the size is $1^\circ \times 1^\circ$ and the spatial resolution is 50 m.

The global forest and nonforest classifications with L -band SAR data were achieved by Shimada *et al.* [9]. The γ^0_{HV} obtained for the same season was mainly used for classifying forest and nonforest areas. The σ^0 over a forest area shows a seasonal/temporal variation. This σ^0 variation caused by the freeze/snow events over a forest area was pointed out by [10]. An

TABLE I
SUMMARY OF THE DATA FROM PALSAR-2 OBSERVATIONS AND FIELD EXPERIMENTS

Year	2016												
Satellite Obs. Cycle*	47	48	—	51	—	53	—	56	—	59	—	61	62
Obs. term	Apr. 25~	May 9~		Jun. 20~		Jul. 18~		Aug. 29~		Oct. 1~		Nov. 7~	Nov. 21~
Scan SAR (Peru)				Jun. 23		Jul. 21		Sep. 1		Oct. 13			
Scan SAR (Brazil)		May 10		Jun. 21		Jul. 19				Oct. 11			
Polarimetry (Peru)	May 5**	May 19***										Nov. 17***	Dec. 1**
Field exp. (Peru)													Nov. 30 to Dec. 2
Air plane Photos(Peru)													Dec. 3

*1 cycle is 14 days **FP6-4 Off-nadir: 28.4° ***FP6-3 Off-nadir: 25.5°.

enhanced L -band backscatter following rainfall events was also reported by [11]. This enhanced L -band backscatter was caused by the enhanced dielectric constant of a tree trunk, which often happens after a rainfall [12].

Almeida-Filho *et al.* [13] used Japanese Earth Resources Satellite 1 (JERS-1) data from the Brazilian Amazon and showed that the σ_{HH}^0 increased in some areas after deforestation. They speculate that the increase in σ_{HH}^0 is due to increased radar reflection from branches and stems lying on the ground. Reiche *et al.* [14] used a Phased Array type L -band SAR (PAL-SAR) time series of approximately two observations per year of data and examined how the PALSAR backscatter observables (HV, HH, HVHH-ratio) were correlated with the Landsat normalized difference vegetation index for deforestation sites. They concluded that the HVHH-ratio provided the most accurate results. Motohka *et al.* [15] used an annual time series of PALSAR mosaic data to demonstrate the possibility of automatic detection of tropical deforestation in Indonesia. They concluded that γ_{HV}^0 was an effective parameter for deforestation detection when a fixed threshold was used. The accuracy of the method ranged from 72% to 96% (with an average of 87%). The study also concluded that γ_{HH}^0 did not always show systematic changes after deforestation.

There have been few studies, however, that have examined the early-stages of deforestation with frequent observational data. For this research, we used not only optical Landsat data observed every 16 days, but also PALSAR-2/ScanSAR dual polarization (HH and HV) data observed every ~ 1.5 months. PALSAR-2/fully polarimetric data were also used to interpret the radar backscattering mechanism from the early-stage deforestation sites, which were verified by using aerial photos taken 2–16 days after the PALSAR-2 observations.

The radar backscattering mechanisms that indicate early-stage deforestation, which typically only lasts a few months, were examined by combining frequent observation of PALSAR-2/ScanSAR and Landsat data while also simultaneously comparing field experiment and PALSAR-2/fully polarimetric observations.

II. DATA AND ANALYSIS

A. PALSAR-2/ScanSAR Data and the Deforestation Polygon From Landsat Data

Two target areas were set around Pucallpa in Peru and Rio Branco in Brazil, some of the most active deforestation spots

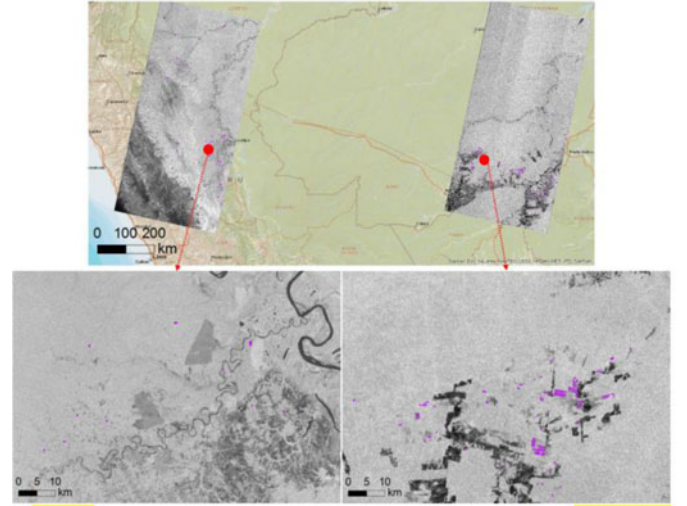


Fig. 1. PALSAR-2/ScanSAR images in Peru (left) observed on June 23, 2016, and Brazil (right) observed on October 11, 2016. The purple polygon represents deforestation sites detected by Landsat (Global Land Analysis & Discovery [3]).

in each country. Four PALSAR-2/ScanSAR datasets obtained between June and October 2016 (satellite observation cycles 51, 53, 56, and 59 [16]) were used in the Peru analysis (see Table I); four PALSAR-2/ScanSAR datasets obtained between May and October 2016 (cycles 48, 51, 53, and 59) were used in the Brazil analysis.

The SAR data were processed by SIGMA-SAR [17] to obtain orthorectified and slope-corrected γ^0 images. The γ^0 is backscattering coefficient per area normal to incidence angle, and obtained from the following formulae.

$$\gamma^0 = \sigma^0 / \cos\theta$$

σ^0 is backscattering coefficient per ground range, and θ is incidence angle.

PALSAR-2/ScanSAR images taken in Peru and Brazil are presented in Fig. 1. Deforestation polygons obtained by the Forest Alerts dataset of GLAD [3] were plotted on the map with purple polygons. Deforestation polygons obtained by GLAD with areas more than 5 ha were used to examine the γ^0 variation during deforestation and afterward.

49 deforestation sites were identified by GLAD between Jun. 20 and Jul. 31 (cycles 51–53) in Peru. Then, the γ^0 change for the deforestation sites, $\Delta\gamma^0$, was examined between cycles 51–53, 53–56, and 56–59. 433 deforestation sites were identified by

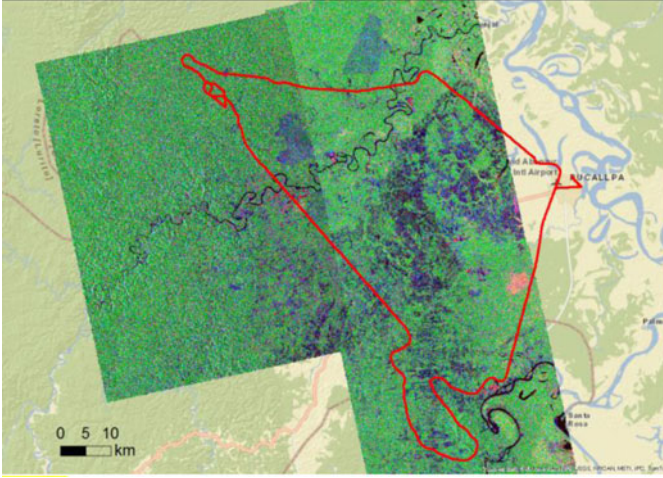


Fig. 2. Four-component decomposition image observed on November 17 (left side) and Dec. 1 (right side), 2016, in Peru. Red, green, and blue colors indicate the areas where double-bounce, volume, and surface scattering, respectively, are dominant. The red line represents the airplane flight course on December 3, 2016.

GLAD between May 10 and Jun. 21 (cycles 48–51) in Brazil. Then, the $\Delta\gamma^0$ was examined between cycles 48–51, 51–53, and 53–59.

B. PALSAR-2/Polarimetry Data

Two PALSAR-2/polarimetry data sets from the Peruvian Amazon were used in this analysis. The areas are included in the ScanSAR observations (see Fig. 1). The first dataset was taken at the beginning of the dry season (May 2016, see Table I), while the second dataset was taken at the end of the dry season (November and December 2016). During the 2016 dry season, significant deforestation occurred in the area. These datasets were used to compare polarimetric characteristics before and after deforestation. The level 1.1 data were processed to examine the radar backscattering mechanisms of early- and later-stage deforestation areas. The parameters included not only σ^0 , but also two representative polarimetric parameters, eigenvalue decomposition [18], and four-component decomposition [19]. Both parameters were obtained using PolSARPro [20].

The eigenvalue decomposition parameters consist of entropy, α , and anisotropy. Entropy represents the randomness of a scatterer, α represents the scattering mechanism (0° for surface scattering, 45° for dipole scattering or single scattering by a cloud of anisotropic particles, and 90° for double-bounce scattering), and anisotropy represents the relative importance of the second and third eigenvalues. The four-component decomposition consists of the surface, volume, double-bounce, and helix scattering components on the Earth's surface.

The processing window size for calculating the parameters was 3×3 pixels. The four-component decomposition image from the end of the dry season is presented in Fig. 2. Red, green, and blue colors indicate the areas where double-bounce, volume, and surface scattering, respectively, are dominant. The

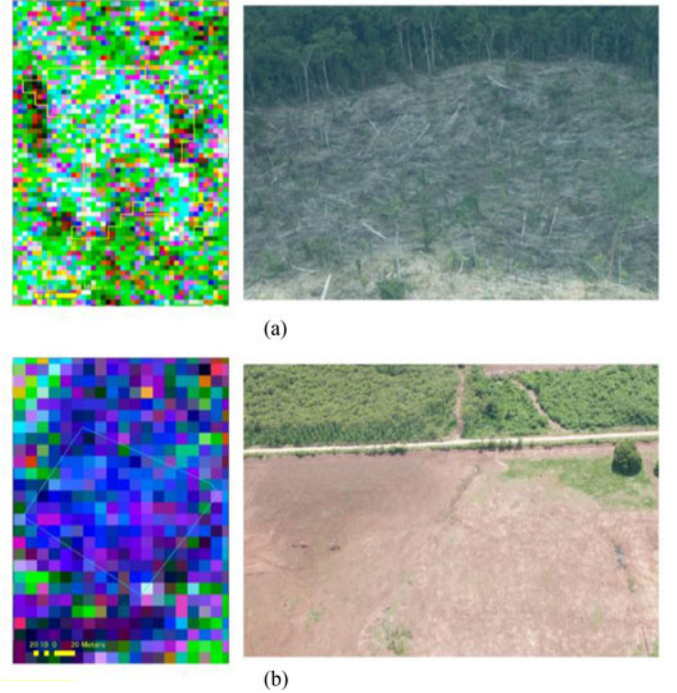


Fig. 3. A four-component decomposition image for the deforestation site (left) and photos taken from the airplane (right) in Peru. (a) Early-stage deforestation site where many felled trees were left on the ground. (b) Site where felled trees were removed and surfaces were flattened.

blue areas are therefore interpreted as regions of deforestation and agriculture, while the green areas are interpreted as forest.

III. FIELD EXPERIMENTS

The field experiments were done from November 30 to December 3, 2016 (see Table I) in Peru. This is the end of the dry season that is similar to the period of the second polarimetric observations. Ground-based field experiments were carried out from November 30 to December 2, 2016 in the southern part of the experimental area in Fig. 2.

Since ground access to the northern part of the area was limited, an airplane was chartered on December 3, 2016 to take photos and videos of the deforestation sites. Using the photos and video, four early-stage deforestation sites, where the many felled trees were left on the ground, were identified [see Fig. 3(a)]. The other two deforestation sites, where felled trees were removed and surfaces were flattened, were also identified [see Fig. 3(b)]. These six sites had been a forest as of May 2016, when the first fully polarimetric observations were completed. The fully polarimetric parameter change between the two observations before and after the deforestation were considered for analysis.

IV. RESULTS AND DISCUSSION

A. Detection Timing

Time series of Sentinel-2 [10 m resolution, false color (urban)] and PALSAR-2 data for a deforestation site are pre-

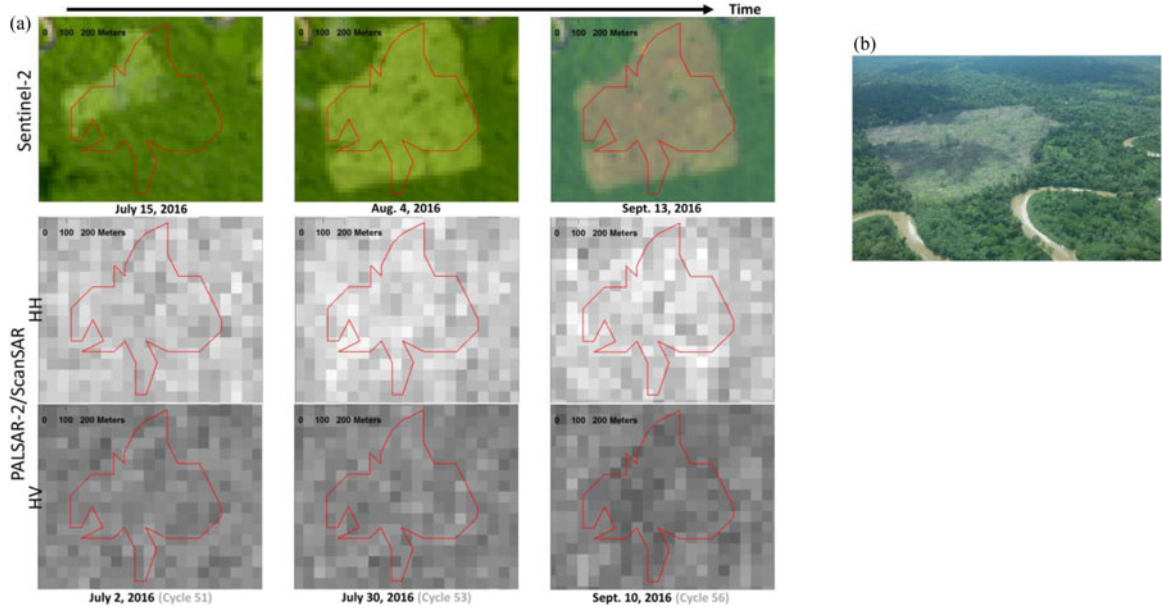


Fig. 4. (a) Time series of Sentinel-2 [false color (urban)] and PALSAR-2/ScanSAR data over a deforestation site. (b) Aerial photo taken on December 3, 2016.

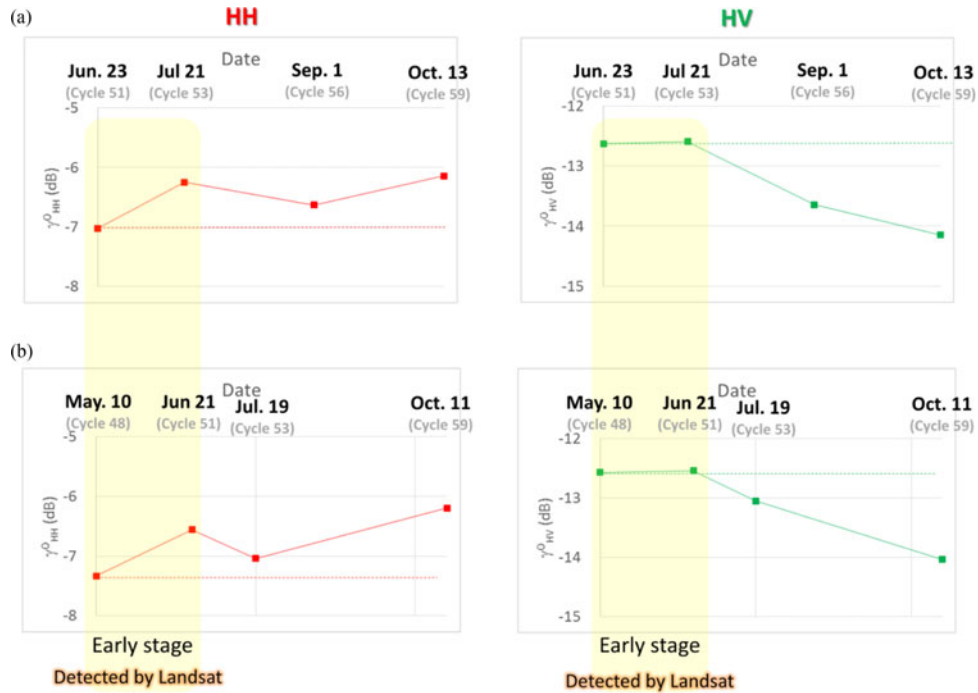


Fig. 5. (a) Temporal variation of averaged γ_{HH}^0 (left) and γ_{HV}^0 (right) for deforestation sites in Peru. (b) Temporal variation of averaged γ_{HH}^0 (left) and γ_{HV}^0 (right) for deforestation sites in Brazil.

sented in Fig. 4. The Sentinel-2 image shows that the region's color changes from dense green (July 15) to light green (August 4), indicating that the trees had felled during this period. The PALSAR-2/HH image becomes bright in this time frame, indicating an increase of γ_{HH}^0 values. The HV image, however, does not show significant change. The HV image becomes dark, indicating a decrease of γ_{HV}^0 on September 10. The aerial pho-

tography on December 3 [see Fig. 4(b)] confirmed that many felled trees had been removed. The temporal variation of averaged γ^0 for deforestation sites in Peru and Brazil is presented in Fig. 5. The deforestation was detected by Landsat between cycles 51–53 for Peru, and cycles 48–51 for Brazil. Many felled trees were expected to be left on the ground in these time periods. The values of γ_{HH}^0 increased by 0.8 dB on average

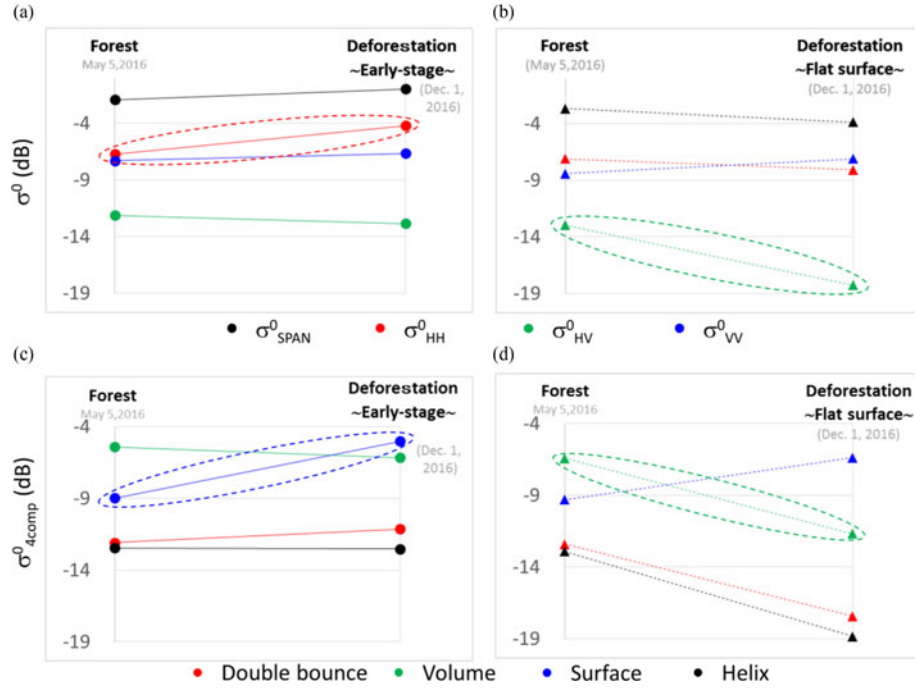


Fig. 6. Polarimetric parameters obtained before and after deforestation for early-stage and flat-surface deforestation sites. (a) σ^0 and (c) four component decomposition parameters obtained from early-stage deforestation sites. (b) σ^0 and (d) four component decomposition parameters obtained from the flat surface deforestation sites.

in both the Peruvian and Brazilian cases. These data support the results obtained by Almeida-Filho *et al.* [13] using JERS-1 HH polarization data from the Brazilian Amazon. On average, the values of γ_{HV}^0 do not change during this time. In the next observation window, the $\Delta\gamma_{HH}^0$ decreased by 0.4 and 0.5 dB, and the $\Delta\gamma_{HV}^0$ decreased by 1.1 and 0.5 dB for Peru and Brazil, respectively. In the next observation window, the $\Delta\gamma_{HH}^0$ increased again by 0.5 and 0.8 dB, while the $\Delta\gamma_{HV}^0$ continued to decrease, dropping by 0.5 and 1.0 dB for Peru and Brazil, respectively. The γ_{HV}^0 decrease 1.6 and 1.5 dB in total 4–5 months after deforestation. It is possible that the branches that were left on the ground, as well as the rough surface, may have increased the γ_{HH}^0 value, despite any removal of felled trees for the later stage deforestation site. The continuous decrease of the γ_{HV}^0 may be explained by the lower sensitivity of the HV polarization to the remaining branches and surface roughness, and higher sensitivity to the forest biomass. In case that only dual polarimetric data (HH and HV polarization) is available, γ_{HH}^0 is a good parameter for detecting early-stage deforestation sites but is not an adequate parameter for detecting later-stage deforestation. Conversely, the parameter γ_{HV}^0 is a useful parameter for detecting later-stage deforestation sites, but not for detecting early-stage deforestation.

B. Polarimetric Characteristics of Deforestation Areas

The polarimetric parameters obtained in the deforestation areas are summarized in Table II, and some of the representative data points obtained with an off-nadir angle of 28.4° are plotted in Fig. 6. The σ_{HH}^0 increased by 1.1–2.5 dB for early-stage deforestation sites, which is consistent with the results obtained with ScanSAR data.

On the other hand, the σ_{HV}^0 decreased by 0.7–1.0 dB for the early-stage deforestation site and 5.2–5.3 dB for the flat surface deforestation site. This finding also supports the ScanSAR results, which indicate continuous decrease of γ_{HV}^0 after deforestation.

Early-stage deforestation sites show larger increase of $\sigma_{surface}^0$, by 2.9–4.0 dB. This can be explained by the increase of direct (single bounce) scattering from felled trees. The 2.9–4.0 dB increase of $\sigma_{surface}^0$ and 0.7 dB decrease of σ_{volume}^0 contribute to a 1.1–2.5 dB increase of σ_{HH}^0 and 0.7–1.0 dB decrease of σ_{HV}^0 for the early-stage deforestation site. The 5.2–5.3 dB and 5.3–5.5 dB decrease of σ_{HV}^0 and σ_{volume}^0 for the deforestation sites with flat surfaces can be explained by less volume and less direct scattering from the surface.

The decrease of entropy indicates less volume scattering, while the decrease of α indicates that the scattering mechanism changed from dipole scattering by a cloud of anisotropic particles to surface scattering after the deforestation. These results also support the conclusion that the scattering mechanism changed in the early-stage deforestation site obtained for the four-component decomposition.

In case that fully polarimetric data is available, surface scattering is a useful parameter for detecting early-stage deforestation sites. γ_{HV}^0 and volume scattering shows same dynamic range for later-stage deforestation site, and are the good parameter for detecting later-stage deforestation sites.

Dual polarimetric observation by PALSAR-2/ScanSAR is scheduled 9th per a year, while fully polarimetric observation is scheduled once per 5-years. Then, using dual polarimetric data (γ_{HH}^0 and γ_{HV}^0) is realistic for early-stage deforestation detection.

TABLE II
POLARIMETRIC PARAMETERS OBTAINED BEFORE AND AFTER DEFORESTATION

	Parameters	Off-nadir: 28.4		Off-nadir: 25.5	
		May 5	Dec 1	May 19	Nov 17
Forest → Early stage	σ_{HH}^0 (dB)	-6.7	-4.2	-5.4	-4.4
	σ_{HV}^0 (dB)	-12.1	-12.9	-11.3	-12.4
	σ_{VV}^0 (dB)	-7.3	-6.7	-6.6	-6.4
	σ_{Span}^0 (dB)	-1.9	-1.0	-1.0	-0.8
	σ_{Double}^0 (dB)	-12.1	-11.1	-11.4	-12.8
	σ_{Volume}^0 (dB)	-5.4	-6.2	-4.6	-5.3
	$\sigma_{Surface}^0$ (dB)	-9.0	-5.0	-8.0	-5.1
	σ_{Helix}^0 (dB)	-12.5	-12.5	-11.4	-12.4
	Entropy	0.8	0.7	0.7	0.6
	α (°)	46.3	41.2	46.3	38.9
	Anisotropy	0.5	0.5	0.5	0.5
Forest → Flat surface	σ_{HH}^0 (dB)	-7.1	-8.1	-5.5	-8.9
	σ_{HV}^0 (dB)	-13.0	-18.3	-12.9	-18.1
	σ_{VV}^0 (dB)	-8.4	-7.1	-7.0	-11.4
	σ_{Span}^0 (dB)	-2.7	-3.9	-1.7	-5.8
	σ_{Double}^0 (dB)	-12.4	-17.4	-11.6	-15.5
	σ_{Volume}^0 (dB)	-6.4	-11.7	-6.1	-11.5
	$\sigma_{Surface}^0$ (dB)	-9.3	-6.4	-7.1	-8.5
	σ_{Helix}^0 (dB)	-12.9	-18.8	-12.8	-17.5
	Entropy	0.8	0.5	0.7	0.6
	α (°)	46.5	26.0	44.5	38.5
	Anisotropy	0.4	0.5	0.5	0.5

V. CONCLUSION

Time series of PALSAR-2/ScanSAR data taken approximately every 1.5 months and Landsat data taken approximately every 16 days were used to examine the differences in the timing of detection of deforestation by different parameters.

For the time period in which the deforestation was detected by Landsat (early-stage deforestation, where many felled trees were left on the ground), the values of γ_{HH}^0 increased, while the values of γ_{HV}^0 do not change. The fully polarimetric data indicates that this can be explained by the strong direct (single bounce) scattering from felled trees left on the ground, and weaker volume scattering from the forest canopy. The γ_{HV}^0 values start to decrease 1–1.5 months after the deforestation detected by Landsat image. The fully polarimetric data indicates that this can be explained by the lower sensitivity of the HV polarization to branches left on the ground and surface roughness and higher sensitivity to the forest biomass. Entropy, and α parameters also support this scenario. These results suggest that γ_{HH}^0 may be a good parameter for detecting early-stage deforestation sites. Conversely, the parameter γ_{HV}^0 may be useful for detecting later-stage deforestation sites.

REFERENCES

- [1] IPCC: Climate change 2014: Mitigation of climate change. *Working Group III Contribution to the Fifth Assessment Report of the Intergovernmental Panel on Climate Change*, New York, NY, USA: Cambridge Univ. Press, 2014.
- [2] J. Lynch, M. Maslin, H. Balzter, and M. Sweeting, "Choose satellites to monitor deforestation," *Nature*, vol. 496, pp. 293–294, Apr. 2013.
- [3] GLAD. [Online]. Available: <http://www.glad.umd.edu>, Accessed on: Jan. 2017.

- [4] M. C. Hansen *et al.*, "Humid tropical forest disturbance alerts using Landsat data," *Environ. Res. Lett.*, vol. 11, 2016, Art. no. 034008.
- [5] PRODES. [Online]. Available: <http://www.obt.inpe.br/OBT/assuntos/programas/amazonia/prodes>, Accessed on: Jan. 2018.
- [6] G. Camara, D. Valeriano, and J. Vianei, "Metodologia para o Cálculo da taxa anual de desmatamento na amazônia legal," [Online]. Available: http://www.obt.inpe.br/prodes/metodologia_TaxaProdes.pdf, pp. 1–37, 2013.
- [7] G. Boeques. [Online]. Available: <http://geobosques.minam.gob.pe/geobosque/view/index.php>, Accessed on: Jan. 2018.
- [8] JJ-FAST. [Online]. Available: http://www.eorc.jaxa.jp/jjfast/jj_index.html, Accessed on: Dec. 2016.
- [9] M. Shimada *et al.*, "New global forest/non-forest maps from ALOS PALSAR data (2007–2010)," *Remote Sens. Environ.*, vol. 155, pp. 13–31, 2014.
- [10] J. B. Way *et al.*, "The effect of changing environmental conditions on microwave signatures of forest ecosystems: Preliminary results of the March 1988 Alaskan aircraft SAR experiment," *Int. J. Remote Sens.*, vol. 11, pp. 1119–1144, 1990.
- [11] R. Lucas *et al.*, "An evaluation of the ALOS PALSAR L-band backscatter — Above ground biomass relationship Queensland, Australia: Impacts of surface moisture condition and vegetation structure," *IEEE J. Sel. Topics Appl. Earth Observ. Remote Sens.*, vol. 3, no. 4, pp. 576–593, Dec. 2010.
- [12] M. Watanabe *et al.*, "Multitemporal fluctuations in L-band backscatter from a Japanese forest," *IEEE Trans. Geosci. Remote Sens.*, vol. 53, no. 11, pp. 5799–5813, Nov. 2015.
- [13] R. Almeida-Filho, A. Rosenqvist, Y. E. Shimabukuro, and J. R. dos Santos, "Evaluation and perspectives of using multitemporal L-Band SAR data to monitor deforestation in the Brazilian Amazônia," *IEEE Geosci. Remote Sens. Lett.*, vol. 2, no. 4, pp. 409–412, Oct. 2005.
- [14] J. Reiche, J. Verbesselt, D. Hoekman, and M. Herold, "Fusing landsat and SAR time series to detect deforestation in the tropics," *Remote Sens. Environ.*, vol. 156, pp. 276–293, 2015.
- [15] T. Motohka, M. Shimada, Y. Uryu, and B. Setiabudi, "Using time series PALSAR gamma nought mosaics for automatic detection of tropical deforestation: A test study in Riau, Indonesia," *Remote Sens. Environ.*, vol. 155, pp. 79–88, 2014.
- [16] PALSAR-2 Basic Observation Scenario. [Online]. Available: <http://www.eorc.jaxa.jp/ALOS-2/en/obs/pal2obsguide.htm>, Accessed on: Jan. 2017.
- [17] M. Shimada, "Verification processor for SAR calibration and interferometry," *Adv. Space Res.*, vol. 23, no. 8, pp. 1477–1486, 1999.
- [18] S. R. Cloude and E. Pottier, "A review of target decomposition theorems in radar polarimetry," *IEEE Trans. Geosci. Remote Sens.*, vol. 34, no. 2, pp. 498–518, Mar. 1996.
- [19] Y. Yamaguchi, T. Moriyama, M. Ishido, and H. Yamada, "Four-component scattering model for polarimetric SAR image decomposition," *IEEE Trans. Geosci. Remote Sens.*, vol. 43, no. 8, pp. 1699–1706, Aug. 2005.
- [20] E. Pottier *et al.*, "Overview of the PolSARpro V4.0 software. The open source toolbox for polarimetric and interferometric polarimetric SAR data processing," in *Proc. IEEE Int. Geosci. Remote Sens. Symp.*, 2009, vol. 4, pp. 936–939.



Manabu Watanabe (SM'14) received the B.Sc. degree in physics from Shinsyu University, Nagano, Japan, in 1991, and the Ph.D. degree in astrophysics by using Japanese X-ray astronomy satellite data from Nagoya University, Nagoya, Japan, in 2000.

He was a Researcher with the Japan Aerospace Exploration Agency (JAXA), where he was a part of the Daichi data analysis group. At Tohoku University, between 2007 and 2011, he developed a ground-based scatterometer system, and examined the radar reflection from permafrost. At JAXA, between 2011 and

2016, his primary duty was analyzing SAR data for understanding radar scattering from forests and disaster areas. He is currently with Tokyo Denki University, Tokyo, Japan. His primary duty is developing forest deforestation algorithm for JICA-JAXA Forest Early Warning System in the Tropics. He has authored or coauthored several conference papers and is a Member of the Remote Sensing Society of Japan.



Christian N. Koyama (M'09) received the Dipl. degree and the Ph.D. degree (Hons.) in physical geography and remote sensing from the University of Cologne, Cologne, Germany, in 2007 and 2012, respectively.

From 2013 to 2016, he was a Postdoctoral Research Fellow with the Center for Northeast Asian Studies, Tohoku University, where he developed a polarimetric UWB GB-SAR system for the detection of earthquake-induced damages in wooden structures.

Since June 2016, he has been an Assistant Professor with the School of Science and Engineering, Tokyo Denki University. As a JICA- Japan Aerospace Exploration Agency Project Researcher, he is currently involved in the development of an ALOS-2 based early warning system to battle deforestation in the tropics. His main research interests include radar remote sensing, including quantitative parameter estimation for geoscience applications and disaster mitigation, radar polarimetry, near-range imaging, and stereo-SAR.



Masato Hayashi received the B.Sc. and M.Sc. degrees in geophysics, and studied a high-resolution infrared spectrometer to observe the planetary atmosphere, from Tohoku University, Sendai, Japan, in 1994 and 1996, respectively, and the Ph.D. degree in agronomy, and studied space-borne LiDAR applications for forest resources assessment, from Hokkaido University, Sapporo, Japan, in 2015.

From 1997 to 2011, he was with Asia Air Survey Co., Ltd., and with Japan Forest Technology Association to develop remote sensing technology for forestry. From 2011 to 2016, he was a Researcher with the National Institute for Environmental Studies. Since 2016, he has been an Associate Senior Researcher with Japan Aerospace Exploration Agency (JAXA), and developing JICA-JAXA forest early warning system in the tropics to prevent deforestation in the tropics. His current research interest focuses on remote sensing technology for large-scale forest resources observation using active satellite sensors: SAR and LiDAR.

Izumi Nagatani received the Ph.D. degree in information science from Tohoku University, Sendai, Japan, in 2014.

He is a System Engineer for GIS, remote sensing, and satellite image real-time processing systems. He was with the Forestry and Forest Products Research Institute, Japan, during 1995–2001, with the National Institute for Agro-Environmental Sciences in 2002, and with Nippon Hakuyo Electronics, Ltd., during 2003–2014. He has experience in RS studies for forestry and agriculture using Landsat, SPOT, and aerial hyperspectral image data, and has developed early warning systems, which were forest fire detection systems using NOAA, DMSP (for ANDES project), and MODIS data (for AFFIRE project), and a drought monitoring system for agriculture, while maintaining an X-band reception system for MODIS and a satellite image database system of the Ministry of Agriculture, Forestry and Fisheries of Japan. He also developed a transboundary air pollution monitoring system in 2011–2014 with Tohoku University. Then he was with Advanced Industrial Science and Technology as a Postdoctoral Researcher. Since 2016, he has been with Japan Forest Technology Association and is working for Japan Aerospace Exploration Agency (JAXA) for developing the JICA-JAXA Forest Early Warning System in the Tropics.

Dr. Nagatani is a member of the Remote Sensing Society of Japan and the Japan Society of Photogrammetry and Remote Sensing.



Masanobu Shimada (M'97–SM'04–F'11) received the B.S. and M.S. degrees in aeronautical engineering from Kyoto University, Kyoto, Japan, in 1977 and 1979, and the Ph.D. degree in electrical engineering from the University of Tokyo, Tokyo, Japan, in 1999.

In 1979, he joined the National Space Development Agency of Japan [NASDA, former Japan Aerospace Exploration Agency (JAXA)] and remained there for 34 years. During that time, he worked on the JERS-1 SAR calibration and validation (1992–1998), the JERS-1 Science Project (Global Rainforest and Boreal Forest Mapping Project and SAR Interferometry Project), the development of a polarimetric airborne SAR (Pi-SAR-L), the PALSAR CALVAL, and the Kyoto and Carbon Initiative Project using the time-series PALSAR/PALSAR2 mosaics. His main outputs are the world's first global SAR mosaics showing annual deforestation change and large-scale land surface deformations. His current research interests include high-resolution imaging for spaceborne and airborne SARs (PALSAR-2 and Pi-SAR-L2), calibration and validation, and SAR applications including polarimetric SAR interferometry. Since April 1, 2015, he has been a Professor with Tokyo Denki University, Tokyo, Japan, an invited Researcher with JAXA, and a Guest Professor with Yamaguchi University, Yamaguchi, Japan.